mathematics

Review

A Fitted Operator Finite Difference Approximation for Singularly Perturbed Volterra–Fredholm Integro-Differential Equations

Musa Cakir *,† and Baransel Gunes †

Department of Mathematics, Faculty of Science, Van Yuzuncu Yil University, Van 65080, Turkey
* Correspondence: musacakir@yyu.edu.tr
† These authors contributed equally to this work.

Abstract: This paper presents a ε-uniform and reliable numerical scheme to solve second-order singularly perturbed Volterra–Fredholm integro-differential equations. Some properties of the analytical solution are given, and the finite difference scheme is established on a non-uniform mesh by using interpolating quadrature rules and the linear basis functions. An error analysis is successfully carried out on the Boglaev–Bakhvalov-type mesh. Some numerical experiments are included to authenticate the theoretical findings. In this regard, the main advantage of the suggested method is to yield stable results on layer-adapted meshes.

Keywords: error analysis; finite difference method; Fredholm integro-differential equation; singular perturbation; Volterra integro-differential equation; uniform convergence

MSC: 65L10; 65L11; 65L12; 65L20; 65R20

Citation: Cakir, M.; Gunes, B. A Fitted Operator Finite Difference Approximation for Singularly Perturbed Volterra–Fredholm Integro-Differential Equations. *Mathematics* **2022**, *10*, 3560. https://doi.org/10.3390/math10193560

Academic Editor: Mirosław Lachowicz

Received: 7 September 2022
Accepted: 21 September 2022
Published: 29 September 2022
Corrected: 13 December 2022

1. Introduction

Volterra–Fredholm integro-differential equations (VFIDEs) have led to many scientific computings. They play important roles in different branches of science involving aerodynamics, the economy, electricity and electronics, industrial networks, hydrodynamics, oceanography and chemistry [1–3] (see the references detailed within). Particularly, VFIDEs have been used widely for population growth, medicine processes and pandemic research. For example, the dissipation of tumor cells and the response of immune system were modeled in [4]. The effect of the COVID-19 pandemic was investigated in Italy, Germany and France with the help of modeling by some integro-differential equations [5,6].

Some existence and uniqueness results for VFIDEs have been presented by Hamoud and his co-authors in [7,8]. Due to their importance in computational science, numerous methods have been introduced for solving VFIDEs. Various semi-analytical techniques including Adomian decomposition method, variational iteration method, homotopy perturbation method, modified differential transform method and Laplace decomposition method have been proposed in [2,9,10]. Furthermore, many scholars have developed different numerical approaches. These include the exponential spline method [11], the collocation method [1], the Nyström method [12], reproducing the kernel method [13], the Haar wavelet [14,15], the Chebyshev–Galerkin method [16], the operational matrix method of Bernstein polynomials [17], the finite difference method [18,19], the Galerkin method [20,21], the bezier curve method [22], etc. [3,23–26]. The mentioned studies have only dealt with regular cases (i.e., absent the singularity).

This article concerns with boundary-value problem of second-order Volterra–Fredholm integro-differential equation in the form

$$Lu + Tu + Su = f(x),\ x \in \bar{I}, \tag{1}$$

subject to boundary conditions

$$u(0) = A,\ u(l) = B, \tag{2}$$

in which the differential operator Lu, the Volterra integral operator T and the Fredholm integral operator S are given as follow, respectively:

$$Lu = -\varepsilon^2 u'' + a(x)u,\ Tu = \lambda \int_0^x K_1(x,t)u(t)dt$$

and

$$Su = \lambda \int_0^l K_2(x,t)u(t)dt.$$

Additionally, $\varepsilon \in (0,1]$ is a small parameter, $\bar{I} = [0,l]$, λ is a real parameter, the functions $a(x) \geq \alpha > 0$, $f(x)$ $(x \in \bar{I})$, $u(x)$ $(x \in \bar{I})$, $K_1(x,t)$ and $K_2(x,t)$ $((x,t) \in \bar{I} \times \bar{I})$ are sufficiently smooth. Under these conditions, the problem (1) and (2) has unique solution u. As ε tends toward zero, the boundary layers appear in neighborhood of $x = 0$ and $x = l$.

In recent times, a lot of papers have been published about singularly perturbed integro-differential equations and various numerical schemes have been suggested. Iragi and Munyakazi have considered fitted operator finite difference method by using right-side rectangle rule and trapezoidal integration on Shishkin mesh for Volterra integro-differential equations with singularity [27,28]. In [29–31], Volterra delay integro-differential equations with initial layer have been investigated on uniform mesh. Mbroh et. al. have proposed non-standard finite difference scheme by using composite Simpson's rule. Additionally, they have improved the order of convergence by applying Richardson extrapolation [32]. In [33], second-order discretization have been presented on piecewise uniform mesh. Tao and Zhang have introduced the coupled method involving local discontinuous Galerkin technique and continuous finite element method in [34]. In [35], using composite trapezoidal rule, fitted mesh finite difference schemes have been established on Shishkin type mesh. Moreover, almost second-order accuracies for the presented method have been obtained. Exponentially fitted difference schemes have been suggested for singularly perturbed Fredholm integro-differential equations in [36–38]. In [39], Durmaz and Amiraliyev have constructed fitted second-order homogeneous difference scheme on Shishkin mesh for Fredholm integro differential equations with layer behavior. Authors in [40,41] have presented a new discrete scheme for singularly perturbed Volterra-Fredholm integro-differential equations.

To the best of our knowledge, the problems in (1) and (2) have not been investigated using the finite difference schemes. Therefore, this study aims to fill this gap. This paper introduces the new difference scheme for the boundary value problems of second-order singularly perturbed Volterra–Fredholm integro-differential equations as the major novelty of this work. The second contribution is the convergence analysis of the presented scheme on Boglaev–Bakhvalov-type mesh. Last but not least, the proposed algorithm is easy to construct, and it provides stable results in a short time in terms of computation. From these objectives, the theory and applications of the presented method have been extensively studied.

The remainder of this article is organized is as follows. In Section 2, first, some preliminary results are given. Then, using composite numerical quadrature rules and implicit difference rules, the finite difference scheme is constructed on Boglaev–Bakhvalov-type mesh in Section 3. Section 4 is devoted to error approximations and stability analysis. In Section 5, three numerical examples are solved by the proposed method. Furthermore, the corresponding algorithm and the computational results are presented. Finally, the paper ends with "Concluding Remarks".

2. Asymptotic Properties

This section is devoted to some a priori bounds. For this aim, the following lemma is expressed.

Lemma 1. *We assume that* $a, f \in C^1[0,l]$, $\frac{\partial^s K_1}{\partial x^s} \in C[0,l]^2$, $\frac{\partial^s K_2}{\partial x^s} \in C[0,l]^2$, $(s = 0,1)$, $\bar{K}_1 = \max_{\bar{I}\times\bar{I}} |K_1(x,t)|$, $\bar{K}_2 = \max_{\bar{I}\times\bar{I}} |K_2(x,t)|$ *and*

$$|\lambda| < \frac{\alpha}{\max\limits_{0\le x\le l} \int_0^x |K_1(x,t)|dt + \max\limits_{0\le x\le l} \int_0^l |K_2(x,t)|dt}. \tag{3}$$

Then, the solution $u(x)$ *of the problems in* (1) *and* (2) *holds*

$$\|u\|_\infty \le C_0 \tag{4}$$

and

$$|u'(x)| \le C\left\{1 + \frac{1}{\varepsilon}\left(e^{\frac{-\sqrt{\alpha}x}{\varepsilon}} + e^{\frac{-\sqrt{\alpha}(l-x)}{\varepsilon}}\right)\right\},\ 0 < x < l, \tag{5}$$

where

$$C_0 = (1-\gamma)^{-1}\left(|A| + |B| + \alpha^{-1}\|f\|_\infty\right)$$

and

$$\gamma = \alpha^{-1}|\lambda| \max_{0\le x\le l} \int_0^x |K_1(x,t)|dt + \alpha^{-1}|\lambda| \max_{0\le x\le l} \int_0^l |K_2(x,t)|dt < 1.$$

Proof. By considering the maximum principle for the problems in (1)–(2), we obtain

$$\begin{aligned} |u(x)| \quad &\le \quad |A| + |B| + \alpha^{-1} \max_{0\le x\le l} |f(x)| + \alpha^{-1}|\lambda| \max_{0\le x\le l} \int_0^x |K_1(x,t)||u(t)|\,dt \\ &\quad +\alpha^{-1}|\lambda| \max_{0\le x\le l} \int_0^l |K_2(x,t)||u(t)|dt. \end{aligned}$$

Then, it follows that

$$\begin{aligned} \|u\|_\infty \le |A| + |B| + \alpha^{-1}\|f\|_\infty + \alpha^{-1}|\lambda| \max_{0\le x\le l} \int_0^x |K_1(x,t)|dt\|u\|_\infty \\ +\alpha^{-1}|\lambda| \max_{0\le x\le l} \int_0^l |K_2(x,t)|dt\|u\|_\infty. \end{aligned}$$

Finally, we have

$$\|u\|_\infty \le (1-\gamma)^{-1}\left(|A| + |B| + \alpha^{-1}\|f\|_\infty\right).$$

By taking into consideration (3), we reach the proof of the (4). Now, we prove the relation (5). Since $|K_1| \le \bar{K}_1$, $|K_2| \le \bar{K}_2$ and $|u(x)| \le C$, we can write for the second derivative of $u(x)$

$$|u''(x)| \le \frac{1}{\varepsilon^2}[|f(x)| + |a(x)||u(x)|$$

$$+|\lambda|\int_0^x |K_1(x,t)||u(t)|dt + |\lambda|\int_0^l |K_2(x,t)||u(t)|dt\Bigg] \leq \frac{C}{\varepsilon^2},\ 0 \leq x \leq l.$$

For any function $g \in C^2[0,l]$, the following formula is used to estimate $|u'(0)|$ and $|u'(l)|$:

$$g'(x) = g[\alpha_0, \alpha_1] - \int_{\alpha_0}^{\alpha_1} K_0(\xi, x)g''(\xi)d\xi,\ \alpha_0 < \alpha_1, \tag{6}$$

where

$$g[\alpha_0, \alpha_1] = \frac{g(\alpha_1) - g(\alpha_0)}{\alpha_1 - \alpha_0},$$

$$K_0(\xi, x) = T_0(\xi - x) - (\alpha_1 - \alpha_0)^{-1}(\xi - \alpha_0)$$

and

$$T_0(\lambda) = \begin{cases} 1, & \lambda \geq 0, \\ 0, & \lambda < 0. \end{cases}$$

In (6), by taking $g(x) = u(x),\ x = 0,\ \alpha_0 = 0$ and $\alpha_1 = \varepsilon$, we find the estimation of $|u'(0)|$:

$$|u'(0)| \leq \frac{u(\varepsilon) - u(0)}{\varepsilon} - \int_0^\varepsilon K_0(\xi, 0)u''(\xi)d\xi \leq \frac{C}{\varepsilon}.$$

In the same way, rewriting $g(x) = u(x),\ x = l,\ \alpha_0 = l - \varepsilon$ and $\alpha_1 = l$ in (6), we obtain

$$|u'(l)| \leq \frac{u(l) - u(\varepsilon)}{\varepsilon} - \int_{l-\varepsilon}^{l} K_0(\xi, l)u''(\xi)d\xi \leq \frac{C}{\varepsilon}.$$

Differentiating (1), we have

$$-\varepsilon^2 v'' + a(x)v = F(x), \tag{7}$$

$$v(0) = O(\frac{1}{\varepsilon}),\ v(l) = O(\frac{1}{\varepsilon}). \tag{8}$$

From (4), it is clear that

$$|F(x)| \leq C. \tag{9}$$

We investigate the solution of the problems in (7) and (8) in the following form:

$$v(x) = v_1(x) + v_2(x),$$

Here, the functions $v_1(x)$ and $v_2(x)$ are the solutions of the following problems, respectively:

$$-\varepsilon^2 v_1'' + a(x)v_1 = F(x), \tag{10}$$

$$v_1(0) = v_1(l) = 0 \tag{11}$$

and

$$-\varepsilon^2 v_2'' + a(x)v_2 = 0, \tag{12}$$

$$v_2(0) = O\left(\frac{1}{\varepsilon}\right),\ v_2(l) = O\left(\frac{1}{\varepsilon}\right). \tag{13}$$

By using the maximum principle, we obtain

$$|v_1(x)| \leq \alpha^{-1}\|F\|_\infty \leq C,\ 0 \leq x \leq l, \tag{14}$$

and

$$|v_2(x)| \leq w(x). \tag{15}$$

Here, the function $w(x)$ is the solution of the following problem:

$$-\varepsilon^2 w''(x) + aw = 0, \tag{16}$$

$$w(0) = |v_2(0)|,\ w(l) = |v_2(l)|. \tag{17}$$

For the solution of the problems in (16) and (17), it is obvious that

$$w(x) = \frac{1}{\sinh\left(\frac{\sqrt{\alpha}l}{\varepsilon}\right)}\left\{w(0)\sinh\left(\frac{\sqrt{\alpha}(l-x)}{\varepsilon}\right) + w(l)\sinh\left(\frac{\sqrt{\alpha}l}{\varepsilon}\right)\right\}.$$

From here, we can write

$$w(x) \leq \frac{C}{\varepsilon}\left\{e^{\frac{-\sqrt{\alpha}x}{\varepsilon}} + e^{\frac{-\sqrt{\alpha}(l-x)}{\varepsilon}}\right\}. \tag{18}$$

Thus, we obtain

$$\left|u'(x)\right| \leq |v_1(x)| + |v_2(x)|,$$

which hints at the proof of the relation (5) [42]. Therefore, the proof of the lemma is completed. □

3. Discrete Scheme

In this section, the finite difference discretization is presented for the problem (1) and (2). First, we give the definition of the mesh. Let ω_N be a non-uniform mesh on $[0,l]$:

$$\omega_N = \{0 < x_1 < x_2 < \dots < x_{N-1},\, h_i = x_i - x_{i-1}\}$$

and

$$\overline{\omega}_N = \omega_N \cup \{x_0 = 0,\ x_N = l\}.$$

Here, we use the non-uniform mesh called Boglaev–Bakhvalov-type mesh in [43]. The transition point is taken as

$$\sigma_1 = \min\{\frac{l}{4}, \alpha^{-1}\varepsilon|\ln\varepsilon|\}.$$

For an even number N, we divide each of the subintervals $[0,\sigma_1], [\sigma_1,\sigma_2]$ and $[\sigma_2, l]$. Here, $\sigma_2 = l - \sigma_1$. x_i node points are specified as

$$x_i = \begin{cases} -\alpha^{-1}\varepsilon\ln\left(1-(1-\varepsilon)\frac{4i}{N}\right),\ i=0,1,\dots,\frac{N}{4},\ x_i\in[0,\sigma_1],\ \sigma_1<\frac{l}{4}; \\ -\alpha^{-1}\varepsilon\ln\left(1-(1-e^{-\frac{\alpha l}{4\varepsilon}})\frac{4i}{N}\right),\ i=0,1,\dots,\frac{N}{4},\ x_i\in[0,\sigma_1],\ \sigma_1=\frac{l}{4}; \\ \sigma_1+(i-\frac{N}{4})h^{(1)},\ i=\frac{N}{4}+1,\dots,\frac{3N}{4},\ x_i\in[\sigma_1,\sigma_2],\ h^{(1)}=\frac{2(\sigma_2-\sigma_1)}{N}; \\ \sigma_2-\alpha^{-1}\varepsilon\ln\left(1-(1-\varepsilon)\frac{4\left(i-\frac{3N}{4}\right)}{N}\right),\ i=\frac{3N}{4}+1,\dots,N,\ x_i\in[\sigma_2,l],\ \sigma_2<\frac{3l}{4}; \\ \sigma_2-\alpha^{-1}\varepsilon\ln\left(1-(1-e^{-\frac{\alpha l}{4\varepsilon}})\frac{4\left(i-\frac{3N}{4}\right)}{N}\right),\ i=\frac{3N}{4}+1,\dots,N,\ x_i\in[\sigma_2,l],\ \sigma_2=\frac{3l}{4}. \end{cases}$$

Before constructing the difference scheme, we define some notation for the mesh functions. For any mesh function $v(x)$ defined on $\bar{\omega}_N$, we use the following implicit difference rules:

$$v_i = v(x_i),\ v_{\bar{x},i} = \frac{v_i - v_{i-1}}{h_i},$$

$$v_{x,i} = \frac{v_{i+1} - v_i}{h_{i+1}},\ v_{\bar{x}\hat{x},i} = \frac{1}{\hbar_i}(v_{x,i} - v_{\bar{x},i}).$$

Here, $\hbar_i$ is defined as

$$\hbar_i = \frac{1}{2}(h_i + h_{i+1})$$

and the discrete maximum norm is denoted by

$$\|v\|_\infty = \|v\|_{\infty,\bar{\omega}_N} = \max_{0\le i\le N}|v_i|.$$

To establish the difference scheme for the problems in (1) and (2), we use the following integral identity:

$$\hbar_i^{-1}\int_{x_{i-1}}^{x_{i+1}}[Lu+Tu+Su]\varphi_i(x)dx = \hbar_i^{-1}\int_{x_{i-1}}^{x_{i+1}} f(x)\varphi_i(x)dx,\ i=1,2,...,N-1, \tag{19}$$

where the basis function is defined as follows:

$$\varphi_i(x) = \begin{cases} \varphi_i^{(1)}(x) = \frac{x-x_{i-1}}{h_i}, & x\in(x_{i-1},x_i) \\ \varphi_i^{(2)}(x) = \frac{x_{i+1}-x}{h_{i+1}}, & x\in(x_i,x_{i+1}) \\ 0, & x\notin(x_{i-1},x_{i+1}). \end{cases}$$

Moreover, it can be easily seen that

$$\hbar_i^{-1}\int_{x_{i-1}}^{x_{i+1}}\varphi_i(x)dx = \hbar_i^{-1}\left(\frac{h_i}{2}+\frac{h_{i+1}}{2}\right) = 1.$$

For the differential operator Lu in (19), after using interpolating quadrature rules in [44] and some manipulations, we find

$$\begin{aligned}\hbar_i^{-1}\int_{x_{i-1}}^{x_{i+1}} Lu\varphi_i(x)dx &= \hbar_i^{-1}\varepsilon^2\int_{x_{i-1}}^{x_i} u'\varphi_i^{(1)'}(x)dx + \hbar_i^{-1}\varepsilon^2\int_{x_i}^{x_{i+1}} u'\varphi_i^{(2)'}(x)dx \\ &+a_i\hbar_i^{-1}\int_{x_{i-1}}^{x_i} u(x)\varphi_i^{(1)}(x)dx + a_i\hbar_i^{-1}\int_{x_i}^{x_{i+1}} u(x)\varphi_i^{(2)}(x)dx \\ &= L_h u_i + R_i^{(1)} + R_i^{(2)},\end{aligned} \tag{20}$$

where

$$L_h u_i = -\varepsilon^2 u_{\bar{x}\hat{x},i} + a_i u_i,$$

$$R_i^{(1)} = -\hbar_i^{-1}\int_{x_{i-1}}^{x_{i+1}}[a(x)-a(x_i)]u(x)\varphi_i(x)dx \tag{21}$$

and

$$R_i^{(2)} = \hbar_i^{-1}\int_{x_{i-1}}^{x_{i+1}} dx\varphi_i(x)\int_{x_{i-1}}^{x_{i+1}}\frac{du(\xi)}{d\xi}T_0(x-\xi)d\xi.$$

Here, for $s=0$, T_0 is computed as

$$T_s(\lambda) = \begin{cases} \frac{\lambda^s}{s!}, & \lambda\ge 0; \\ 0, & \lambda<0. \end{cases}$$

Moreover, for the right-side of the relation (19), we obtain

$$\hbar_i^{-1}\int_{x_{i-1}}^{x_{i+1}} f(x)\varphi_i(x)dx = f_i + R_i^{(3)} \tag{22}$$

with the remainder term given by

$$R_i^{(3)} = \hbar_i^{-1}\int_{x_{i-1}}^{x_{i+1}} [f(x)-f(x_i)]\varphi_i(x)dx. \tag{23}$$

For the Volterra operator in the relation (19), using interpolating quadrature rules in [44], we obtain

$$\begin{aligned}\hbar_i^{-1}\int_{x_{i-1}}^{x_{i+1}} Tu\varphi_i(x)dx &= \lambda\hbar_i^{-1}\int_{x_{i-1}}^{x_{i+1}} dx\varphi_i(x)\int_0^x K_1(x,t)u(t)dt \\ &= \lambda\int_0^x K_1(x_i,t)u(t)dt + R_i^{(4)}\end{aligned}$$

where

$$R_i^{(4)} = -\hbar_i^{-1}\lambda\int_{x_{i-1}}^{x_{i+1}} dx\varphi_i(x)\int_{x_{i-1}}^{x_{i+1}}\left(\int_0^x \frac{\partial}{\partial x}K_1(x,t)u(t)dt\right)dx. \tag{24}$$

After applying the composite right side rectangle rule, we have

$$\lambda\int_0^x K_1(x_i,t)u(t)dt + R_i^{(4)} = \lambda\sum_{j=1}^{i}\hbar_j K_{1,ij}u_j + R_i^{(4)} + R_i^{(5)},$$

where

$$R_i^{(5)} = -\lambda\sum_{j=1}^{i}\int_{x_{j-1}}^{x_j}(\xi - x_{j-1})\left(\int_0^x \frac{\partial}{\partial\xi}K_1(\xi,t)u(t)dt\right)d\xi. \tag{25}$$

Then, we can write that

$$\hbar_i^{-1}\int_{x_{i-1}}^{x_{i+1}} Tu\varphi_i(x)dx = T_h u_i + R_i^{(4)} + R_i^{(5)}. \tag{26}$$

Here,

$$T_{h_i}u_i = \lambda\sum_{j=1}^{i} h_j K_{1,ij}u_j.$$

Similarly, for the Fredholm operator in the relation (19), applying the interpolating quadrature rules in [44] and the composite right side rectangle rule, it is found that

$$\hbar_i^{-1}\int_{x_{i-1}}^{x_{i+1}} Su\varphi_i(x)dx = S_h u_i + R_i^{(6)} + R_i^{(7)}, \tag{27}$$

where

$$S_h u_i = \lambda\sum_{j=1}^{N}\hbar_j K_{2,ij}u_j,$$

$$R_i^{(6)} = -\hbar_i^{-1}\lambda \int\limits_{x_{i-1}}^{x_{i+1}} dx\varphi_i(x) \int\limits_{x_{i-1}}^{x_{i+1}} \left(\int\limits_0^l \frac{\partial}{\partial x} K_2(x,t)u(t)dt \right) dx$$

and

$$R_i^{(7)} = -\lambda \sum_{j=1}^{N} \int\limits_{x_{j-1}}^{x_j} (\xi - x_{j-1}) \left(\int\limits_0^l \frac{\partial}{\partial \xi} K_2(\xi,t)u(t)dt \right) d\xi.$$

Combining (20), (22), (26) and (27), the following difference scheme is written for the problems in (1) and (2):

$$L_h u_i + T_h u_i + S_h u_i + R_i = f_i,\ 1 \le i \le N-1, \tag{28}$$

where

$$R_i = \sum_{k=1}^{7} R_i^{(k)}. \tag{29}$$

By omitting the error term R_i in (28), we present the following difference problem for the approximate solution:

$$L_h y_i + T_h y_i + S_h y_i = f_i,\ 1 \le i \le N-1, \tag{30}$$

$$y_0 = A,\ y_N = B, \tag{31}$$

where

$$L_h y_i = -\varepsilon^2 y_{\bar{x}\hat{x},i} + a_i y_i,\ T_h y_i = \lambda \sum_{j=1}^{i} \hbar_j K_{1,ij} y_j$$

and

$$S_h y_i = \lambda \sum_{j=1}^{N} \hbar_j K_{2,ij} y_j.$$

4. The Stability and Convergence

Let the error function $z_i = y_i - u_i$, $i = 0,1,2,\dots,N$ be the solution of the following problem:

$$L_h z_i + T_h z_i + S_h z_i = R_i,\ 1 \le i \le N-1 \tag{32}$$

$$z_0 = 0,\ z_N = 0. \tag{33}$$

Here,

$$L_h z_i = -\varepsilon^2 z_{\bar{x}\hat{x},i} + a_i z_i,\ T_h z_i = \lambda \sum_{j=1}^{i} \hbar_j K_{1,ij} z_j,$$

$$S_h z_i = \lambda \sum_{j=1}^{N} \hbar_j K_{2,ij} z_j,$$

and the remainder term R_i is denoted by (29).

Lemma 2. *If*

$$|\lambda| < \frac{\alpha}{\max\limits_{1\le i\le N} \sum_{j=1}^{i} \hbar_j |K_{1,ij}| + \max\limits_{1\le i\le N} \sum_{j=1}^{N} \hbar_j |K_{2,ij}|},$$

the solution of the problem (32) and (33) satisfies that

$$\|z\|_{\infty,\overline{\omega}_N} \le c_0 \|R\|_{\infty,\omega_N},$$

where

$$c_0 = \frac{\alpha^{-1}}{1 - \alpha^{-1}|\lambda| \left(\max\limits_{1 \le i \le N} \sum_{j=1}^{i} \hbar_j |K_{1,ij}| + \max\limits_{1 \le i \le N} \sum_{j=1}^{N} \hbar_j |K_{2,ij}| \right)}.$$

Proof. Applying the discrete maximum principle to the discrete problem (32) and (33), we get

$$|z_i| \le \alpha^{-1} \max_{1 \le i \le N} |R_i| + \alpha^{-1} |\lambda| \max_{1 \le i \le N} \sum_{j=1}^{i} \hbar_j |K_{1,ij}| |z_j| + \alpha^{-1} |\lambda| \max_{1 \le i \le N} \sum_{j=1}^{N} \hbar_j |K_{2,ij}| |z_j|.$$

From here, we can write

$$\|z\|_\infty \le \alpha^{-1} \|R\|_\infty + \alpha^{-1} |\lambda| \max_{1 \le i \le N} \sum_{j=1}^{i} \hbar_j |K_{1,ij}| \|z\|_\infty + \alpha^{-1} |\lambda| \max_{1 \le i \le N} \sum_{j=1}^{N} \hbar_j |K_{2,ij}| \|z\|_\infty.$$

Then, we find

$$\|z\|_\infty (1 - \bar{\gamma}) \le \alpha^{-1} \|R\|_\infty, \tag{34}$$

where

$$\bar{\gamma} = \alpha^{-1} |\lambda| \max_{1 \le i \le N} \sum_{j=1}^{i} \hbar_j |K_{1,ij}| + \alpha^{-1} |\lambda| \max_{1 \le i \le N} \sum_{j=1}^{N} \hbar_j |K_{2,ij}| < 1.$$

Therefore, we arrive at the proof of the lemma. □

Lemma 3. *For the remainder term R_i, the following estimate is satisfied:*

$$\|R\|_{\infty, \omega_N} \le C N^{-1}.$$

Proof. By applying the mean value theorem to function $a(x)$ in $R_i^{(1)}$, we obtain

$$|a(x) - a(x_i)| \le |a'(\xi_i)| |x - x_i| \le C h_i,\ x_i \le \xi_i \le x. \tag{35}$$

Thus, taking into account $a \in C^1[0, l]$ and (35), it is found that

$$\begin{aligned} \left| R_i^{(1)} \right| &\le \hbar_i^{-1} \int_{x_{i-1}}^{x_{i+1}} |a(x) - a(x_i)| |u(x)| |\varphi_i(x)| dx \\ &\le C h_i \hbar_i^{-1} \int_{x_{i-1}}^{x_{i+1}} \varphi_i(x) dx = C h_i. \end{aligned} \tag{36}$$

Similarly, we can write

$$\left| R_i^{(3)} \right| \le C h_i. \tag{37}$$

Additionally, because of the boundedness of T_0 and $|\varphi_i(x)| \le 1$, it is obvious that

$$\left| R_i^{(2)} \right| \le \hbar_i^{-1} \int_{x_{i-1}}^{x_{i+1}} dx |\varphi_i(x)| \int_{x_{i-1}}^{x_{i+1}} \left| \frac{du(\xi)}{d\xi} \right| |T_0(x - \xi)| d\xi \le C h_i. \tag{38}$$

For the remainder term $R_i^{(4)}$, using the Leibnitz rule for the integral term in (24), we have

$$R_i^{(4)} = -\hbar_i^{-1}\lambda \int\limits_{x_{i-1}}^{x_{i+1}} dx\varphi_i(x) \int\limits_{x_{i-1}}^{x_{i+1}} \left(K_1(x,x)u(x) + \int\limits_0^x \frac{\partial}{\partial x} K_1(x,t)u(t)dt \right) dx.$$

Since $\left|\frac{\partial K_1}{\partial x}\right| \leq C$ and $|u(x)| \leq C$, we can find

$$\left|R_i^{(4)}\right| \leq |\lambda| \int\limits_{x_{i-1}}^{x_{i+1}} \left(|K_1(x,x)||u(x)| + \int\limits_0^x \left|\frac{\partial}{\partial x} K_1(x,t)\right| |u(t)|dt \right) dx.$$

Thus, it is seen that

$$\left|R_i^{(4)}\right| \leq Ch_i. \tag{39}$$

In a similar way, we can show

$$\left|R_i^{(6)}\right| \leq Ch_i. \tag{40}$$

For the remainder term $R_i^{(5)}$, applying the Leibnitz rule to the integral term in (25), we obtain

$$\begin{aligned} \left|R_i^{(5)}\right| &\leq |\lambda| \sum_{j=1}^{i} \int\limits_{x_{i-1}}^{x_i} (\xi - x_{j-1}) \left[|K_1(\xi,x)||u(x)| + \int\limits_0^x \left|\frac{\partial}{\partial \xi} K_1(\xi,t)\right| |u(t)|dt \right] d\xi \\ &\leq |\lambda| \int\limits_0^l (\xi - x_{j-1}) \left[|K_1(\xi,x)||u(x)| + \int\limits_0^x \left|\frac{\partial}{\partial \xi} K_1(\xi,t)\right| |u(t)|dt \right] d\xi \\ &\leq C\left\{ h_i + \int\limits_{x_{i-1}}^{x_i} |u'(x)|dx \right\}. \end{aligned} \tag{41}$$

Analogously, we have

$$\left|R_i^{(7)}\right| \leq C\left\{ h_i + \int\limits_{x_{i-1}}^{x_i} |u'(x)|dx \right\}. \tag{42}$$

By substituting (36), (37), (38), (39), (40), (41) and (42) into (29), we estimate that

$$\|R\|_\infty \leq Ch_i.$$

Now, we consider the node points of adaptive mesh. The mesh stepsizes hold

$$h_i = x_i - x_{i-1} \leq CN^{-1},\ h_{i+1} = x_{i+1} - x_i \leq CN^{-1}$$

and

$$\hbar_i = \frac{(h_i + h_{i+1})}{2} \leq CN^{-1}.$$

Then, we estimate the remainder terms for each sub-intervals separately. For the interval $[0, \sigma_1]$, if $\sigma_1 < \frac{l}{4}$, it is found that

$$h_i = x_i - x_{i-1} = \alpha^{-1}\varepsilon\left[\ln\left(1 - (1 - e^{-\frac{\alpha l}{4\varepsilon}})\frac{4i}{N}\right) + \ln\left(1 - (1 - e^{-\frac{\alpha l}{4\varepsilon}})\frac{4(i-1)}{N}\right)\right]$$

$$\leq 4\alpha^{-1}(1-\varepsilon)N^{-1}.$$

Thus, we obtain

$$e^{\frac{-\sqrt{\alpha}x_{i-1}}{\varepsilon}} - e^{\frac{-\sqrt{\alpha}x_{i}}{\varepsilon}} \leq 4\alpha^{-1}(1-\varepsilon)N^{-1}$$

and

$$e^{\frac{-\sqrt{\alpha}(l-x_{i-1})}{\varepsilon}} - e^{\frac{-\sqrt{\alpha}(l-x_{i})}{\varepsilon}} \leq 4\alpha^{-1}(1-\varepsilon)N^{-1}.$$

If $\sigma_1 = \frac{l}{4}$, it can be written that

$$h_i = x_i - x_{i-1} = \alpha^{-1}\varepsilon\left[\ln\left(1-(1-e^{-\frac{\alpha l}{4\varepsilon}})\frac{4i}{N}\right) + \ln\left(1-(1-e^{-\frac{\alpha l}{4\varepsilon}})\frac{4(i-1)}{N}\right)\right]$$
$$\leq \alpha^{-1}(1-\varepsilon)N^{-1} = lN^{-1}.$$

Now, we consider the interval $[\sigma_1, \sigma_2]$. We have

$$h_i = x_i - x_{i-1} = \frac{2(\sigma_2-\sigma_1)}{N} = \frac{2(l-2\sigma_1)}{N} = 2(l-2\sigma_1)N^{-1}.$$

For $\sigma_1 < \frac{l}{4}$, we obtain $h_i \leq lN^{-1}$, and for $\sigma_1 = \frac{l}{4}$, we obtain $h_i = lN^{-1}$. Performing similar operations on the interval $[\sigma_2, l]$, we find

$$|R_i| \leq CN^{-1},$$

which concludes the proof of the lemma. □

Theorem 1. *Let u be the solution of the problems in (1) and (2), and let y be the solution of the discrete problems in (30) and (31). Then, the following estimate is satisfied that*

$$\|y-u\|_{\infty,\overline{\omega}_N} \leq CN^{-1}.$$

Proof. The proof of the theorem can be derived from the previous two lemmas. □

5. Results and Discussion

In this section, we test the numerical method on several examples. For this, the elimination method is used to obtain maximum pointwise errors and convergence rates. Then, the discretization (30) and (31) can be written as the following form:

$$\begin{aligned} A_i y_{i-1} - C_i y_i + B_i y_{i+1} &= -F_i,\ i = 1, \ldots, N-1, \\ y_0 &= A,\ y_N = B. \end{aligned}$$

where

$$\begin{aligned} A_i &= -\varepsilon^2 \hbar_i^{-1} h_i^{-1}, \quad B_i = -\varepsilon^2 \hbar_i^{-1} h_{i+1}^{-1}, \\ C_i &= -\left(\varepsilon^2 \hbar_i^{-1} h_i^{-1} + \varepsilon^2 \hbar_i^{-1} h_{i+1}^{-1} + a_i\right), \\ F_i &= -f_i + \lambda \sum_{j=1}^{i} \hbar_j K_{1,ij} y_j + \lambda \sum_{j=1}^{N} \hbar_j K_{2,ij} y_j. \end{aligned}$$

Here, the coefficients of the elimination method are as follow [45]:

$$\begin{aligned} \alpha_{i+1} &= \frac{B_i}{C_i - \alpha_i A_i},\ \alpha_1 = 0,\ i = 1, \ldots, N-1, \\ \beta_{i+1} &= \frac{F_i + A_i \beta_i}{C_i - \alpha_i A_i},\ \beta_1 = 1,\ i = 1, \ldots, N-1 \end{aligned}$$

and

$$y_i = \alpha_{i+1} y_{i+1} + \beta_{i+1}, \, i = N-1, ..., 1.$$

The corresponding Algorithm 1 is given by

Algorithm 1: To compute the numerical solution y_i.

Input: ε, N, $x(0) = x0$, $x(l) = xN$, $a(x)$, $f(x)$, $K_1(x,t)$, $K_2(x,t)$ and α
Output: The numerical solution y_i
Step 1: $\sigma_1 = sigma1 = min((xN - x0)/4, abs((\varepsilon * reallog(\varepsilon))/\alpha));$
$\sigma_2 = sigma2 = xN - sigma1$
$h^{(1)} = h1 = (sigma2 - sigma1)/(N/2)$
Step 2: for $i = 2 : N+1$
$h_i = h(i) = x(i) - x(i-1)$
$\hbar_i = h2(i) = (h(i+1) + h(i))/2$
end
Step 3: for $i = 2 : N+1$
if $((i <= N/4+1) \&\& (sigma1 < (xN - x0)/4))$
$x(i) = -\varepsilon * reallog(1 - (1-\varepsilon) * 4 * (i-1)/N)/\alpha$
end
if $(i <= N/4+1) \&\& (sigma1 == (xN - x0)/4)$
$x(i) = -\varepsilon * reallog(1 - (1 - exp(-\alpha * xN/(2*\varepsilon))) * 4 * (i-1)/N)/\alpha$
end
if $((i > N/4+1) \&\& (i <= 3*N/4+1))$
$x(i) = sigma1 + h1 * (i - 1 - N/4)$
end
if $((i > 3*N/4+1) \&\& (i <= N))$
$x(i) = xN - x(N+2-i)$
end
end
Step 4: for $i = 2 : N$
$(A_i = A(i), B_i = B(i), C_i = C(i), F_i = F(i), \alpha_i = alfa(i), \beta_i = beta(i))$
$alfa(i+1) = B(i)./(C(i) - alfa(i).*A(i));$
$beta(i+1) = (E(i) + beta(i).*A(i))./(C(i) - alfa(i).*A(i))$
$y(i) = y(i+1).*alfa(i+1) + beta(i+1)$
end

All numerical computations and figures have been carried out by Matlab R2013a. In the numerical experiments, the transition point is chosen as $\sigma_1 \approx 0.25$.

Example 1. *Consider a particular problem*

$$-\varepsilon^2 u'' + u + \int_0^x u(t)dt + \int_0^1 u(t)dt = -\varepsilon\Big(e^{\frac{-x}{\varepsilon}} + e^{\frac{-1}{\varepsilon}} - 2\Big), \; x \in (0,1)$$

$$u(0) = 1, \; u(1) = e^{\frac{-1}{\varepsilon}},$$

in which the exact solution is $u(x) = e^{\frac{-x}{\varepsilon}}$. The nodal maximum errors are specified as

$$e^N = \max_{0 \le i \le N} |y_i - u_i|,$$

where u_i is the exact solution and y_i is approximate solution. Furthermore, the convergence rates are computed as follows

$$p^N = \frac{\ln(e^N/e^{2N})}{\ln 2}.$$

The computed results are presented in Table 1.

Table 1. Maximum pointwise errors e^N and order of convergence p^N on ω_N.

ε	$N = 64$	$N = 128$	$N = 256$	$N = 512$	$N = 1024$
10^{-2}	1.81764×10^{-2} 0.96	9.3384×10^{-3} 0.97	4.73852×10^{-3} 0.98	2.38932×10^{-3} 0.99	$1.200183 - 03$
10^{-4}	2.214777×10^{-2} 0.97	1.137744×10^{-2} 0.98	5.76341×10^{-3} 0.98	2.89803×10^{-3} 0.99	1.45366×10^{-3}
10^{-6}	2.221578×10^{-2} 0.97	1.141305×10^{-2} 0.98	5.78281×10^{-3} 0.99	2.91048×10^{-3} 0.99	1.46022×10^{-3}
10^{-8}	2.432828×10^{-2} 0.97	1.141356×10^{-2} 0.98	5.78307×10^{-3} 0.99	2.91785×10^{-3} 0.99	1.46448×10^{-3}
10^{-10}	2.211679×10^{-2} 0.97	1.141357×10^{-2} 0.98	5.78891×10^{-3} 0.98	2.91269×10^{-3} 0.99	1.46123×10^{-3}
10^{-12}	2.204231×10^{-2} 0.97	1.14026×10^{-2} 0.98	5.7821×10^{-3} 0.99	2.91061×10^{-3} 0.99	1.46007×10^{-3}
e^N p^N	2.432828×10^{-2} 0.96	1.141357×10^{-2} 0.97	5.78891×10^{-3} 0.98	2.91785×10^{-3} 0.99	1.46448×10^{-3}

The behavior of the numerical solution is demonstrated in Figures 1 and 2.

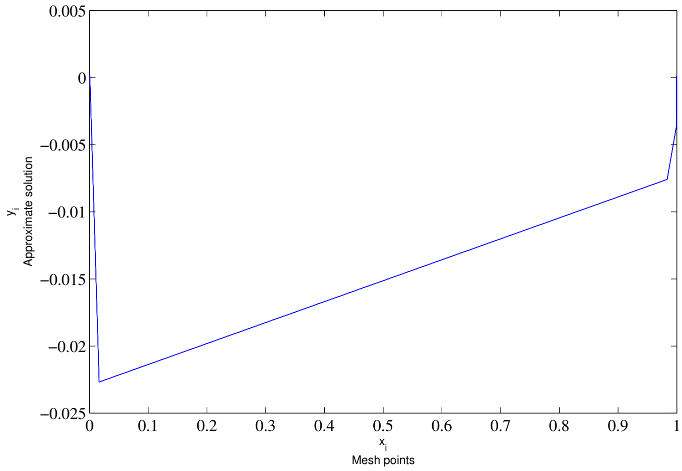

Figure 1. Behavior of the numerical solution for $\varepsilon = 10^{-4}$ and $N = 128$.

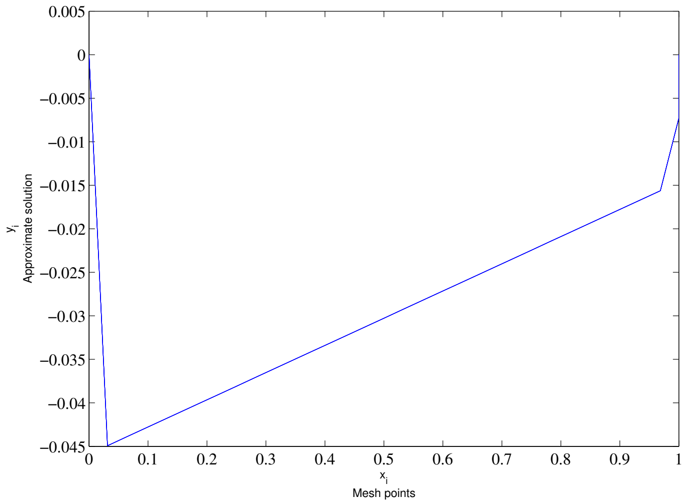

Figure 2. Numerical approximation for $\varepsilon = 10^{-12}$ and $N = 64$.

From Figures 1 and 2, it can be seen that the maximal errors are concentrated within the boundary layers.

Example 2. *We take into account another problem*

$$-\varepsilon^2 u'' + (x+1)u + \frac{1}{2}\int_0^x (1-e^{xt})u(t)dt + \frac{1}{2}\int_0^1 tu(t)dt = \frac{1}{1+x},\ x \in (0,1),$$

$$u(0) = 0,\ u(1) = 1.$$

The exact solution of this equation is unknown. Since the exact solution is unknown, we use the double-mesh technique. The error approximations are indicated by

$$e^N = \max_{0\le i\le N}\left|y_i^N - y_i^{2N}\right|$$

and the order of convergence is defined as follows

$$p^N = \frac{\ln(e^N/e^{2N})}{\ln 2}.$$

Error approximations are shown in Table 2.

Table 2. Maximum pointwise errors e^N and order of convergence p^N on ω_N.

ε	$N=64$	$N=128$	$N=256$	$N=512$	$N=1024$
10^{-2}	2.772958×10^{-2}	1.392083×10^{-2}	6.9501×10^{-3}	3.4764×10^{-3}	1.74087×10^{-3}
	0.99	1.00	1.00	1.00	
10^{-4}	3.289871×10^{-2}	1.64391×10^{-2}	8.21645×10^{-3}	4.10664×10^{-3}	2.05148×10^{-3}
	1.01	1.00	1.00	1.00	
10^{-6}	3.299511×10^{-2}	1.648756×10^{-2}	8.24116×10^{-3}	4.11991×10^{-3}	2.05978×10^{-3}
	1.01	1.00	1.00	1.01	
10^{-8}	3.299655×10^{-2}	1.648829×10^{-2}	8.24152×10^{-3}	4.12113×10^{-3}	2.05604×10^{-3}
	1.00	1.00	1.00	1.00	
10^{-10}	3.299657×10^{-2}	1.648829×10^{-2}	8.24153×10^{-3}	4.12871×10^{-3}	2.05987×10^{-3}
	0.99	0.99	1.00	1.00	
10^{-12}	3.298523×10^{-2}	1.64883×10^{-2}	8.24044×10^{-3}	4.12009×10^{-3}	2.05139×10^{-3}
	1.01	1.00	1.01	1.02	
e^N	3.299657×10^{-2}	1.648830×10^{-2}	8.24153×10^{-3}	4.12871×10^{-3}	2.05987×10^{-3}
p^N	0.99	0.99	1.00	1.00	

The computational results are reflected in the Figures 3 and 4.

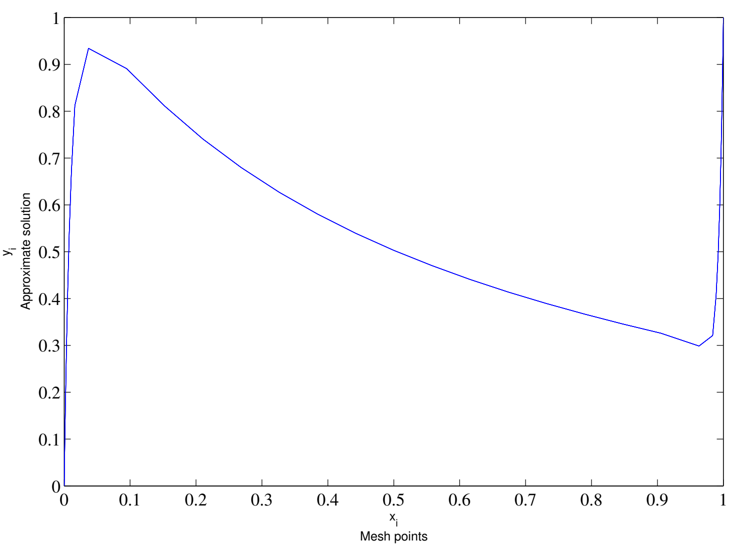

Figure 3. Numerical solution for $\varepsilon = 10^{-2}$ and $N = 32$.

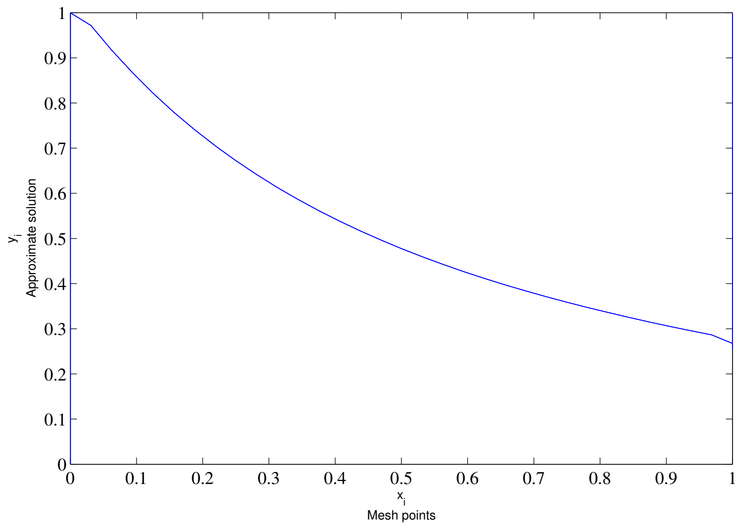

Figure 4. Behavior of the approximate solution for $\varepsilon = 10^{-12}$ and $N = 64$.

In Figures 3 and 4, from $\varepsilon = 10^{-2}$ to $\varepsilon = 10^{-12}$, it is seen that numerical solution behaves stable.

Example 3. *Examine the last problem*

$$-\varepsilon^2 u'' + (1 + e^x)u + \int_0^x \sinh(t)u(t)dt + \int_0^1 \cosh(t)u(t)dt = \sin x - \cos x,\ x \in (0,1),$$

$$u(0) = 0,\ u(1) = e^{\frac{-1}{\varepsilon}} + 1$$

The exact solution of this problem is unknown. Thus, we apply the double-mesh principle again. The obtained results are summarized in Table 3.

Table 3. Maximum pointwise errors e^N and order of convergence p^N on ω_N.

ε	$N = 64$	$N = 128$	$N = 256$	$N = 512$	$N = 1024$
10^{-2}	1.233841×10^{-2}	6.29078×10^{-3}	3.16786×10^{-3}	1.59413×10^{-3}	8.0295×10^{-4}
	0.97	0.99	0.99	0.99	
10^{-4}	1.511043×10^{-2}	7.66589×10^{-3}	3.8615×10^{-3}	1.93738×10^{-3}	9.6936×10^{-4}
	0.98	0.99	0.99	1.00	
10^{-6}	1.516372×10^{-2}	7.69353×10^{-3}	3.87596×10^{-3}	1.90705×10^{-3}	9.3596×10^{-4}
	0.97	0.99	1.02	1.02	
10^{-8}	1.516452×10^{-2}	7.69395×10^{-3}	4.03036×10^{-3}	1.92596×10^{-3}	9.1215×10^{-4}
	0.97	0.93	1.06	1.07	
10^{-10}	1.516453×10^{-2}	7.69487×10^{-3}	4.03738×10^{-3}	1.94571×10^{-3}	9.0143×10^{-4}
	0.98	0.93	1.05	1.11	
10^{-12}	1.516204×10^{-2}	7.69318×10^{-3}	3.83764×10^{-3}	1.9232×10^{-3}	9.0138×10^{-4}
	0.98	1.00	1.00	1.09	
e^N	1.516453×10^{-2}	7.69487×10^{-3}	4.03764×10^{-3}	1.93571×10^{-3}	9.6936×10^{-4}
p^N	0.97	0.93	0.99	0.99	

The improvement in the numerical solution within the boundary layers is illustrated in Figures 5 and 6.

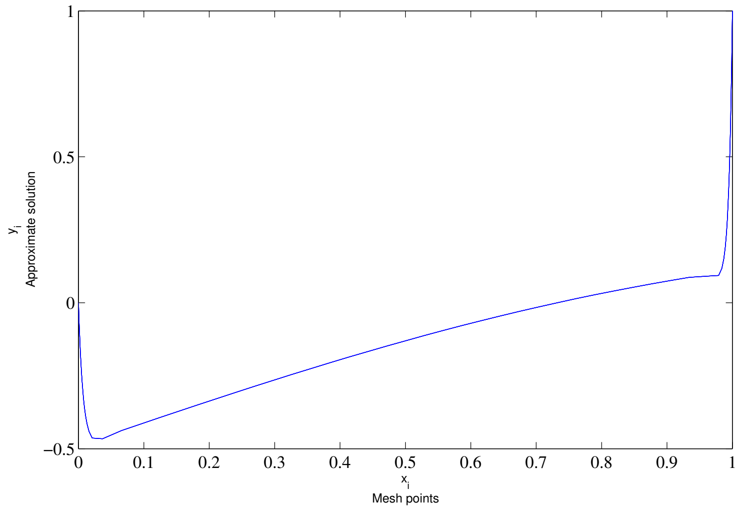

Figure 5. Numerical approximation for $\varepsilon = 10^{-2}$ and $N = 64$.

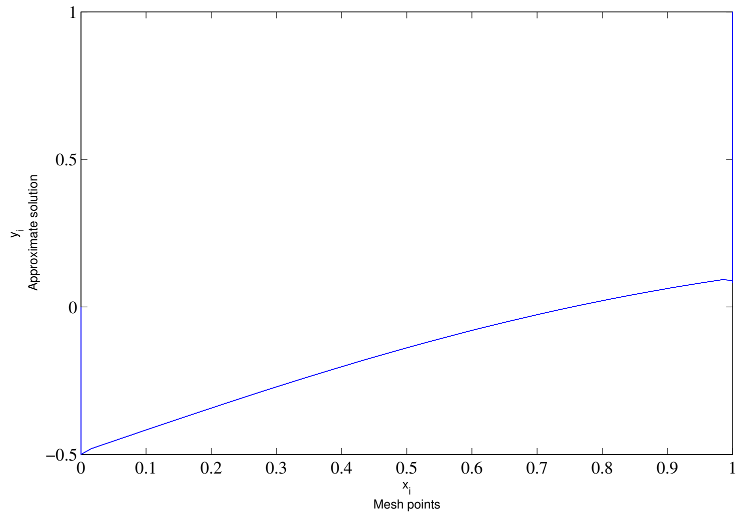

Figure 6. Numerical behavior for $\varepsilon = 10^{-10}$ and $N = 128$.

Figures 5 and 6 show that the numerical solution is treated as ε decreases.

In summary, from Tables 1–3, as N increases, maximum pointwise errors decrease and the order of uniform convergence of the presented difference scheme is almost 1. It can be concluded that the presented difference scheme yields stable and uniform numerical results. Moreover, from Figures 1–6, it is seen that the numerical solution curves converge to the coordinate axes for smaller values of ε. Thus, the proposed method seems to be effective for solving such problems.

6. Concluding Remarks

In this paper, we suggested a new and stable difference scheme for solving boundary value problems of singularly perturbed second-order Volterra–Fredholm integro-differential equations. The stability and convergence of the method were examined in the discrete maximum norm. The effectiveness and reliability of the presented scheme are demonstrated by three numerical examples. The computed results reveal that the order of convergence was found as $O(N^{-1})$. Namely, the scheme is first-order accurate. Although the proposed method is reliable, the order of convergence of the numerical scheme may need to be improved. In order to expand numerical research, experiments in which improvements in the order and different boundary conditions (i.e., nonlocal, integral, Robin, and mixed) can be considered.

Author Contributions: Conceptualization, M.C. and B.G.; methodology, M.C. and B.G.; software, M.C. and B.G.; validation, M.C. and B.G.; formal analysis, M.C. and B.G.; investigation, M.C. and B.G.; resources, M.C. and B.G.; data curation, M.C. and B.G.; writing—original draft preparation, M.C. and B.G.; writing—review and editing, M.C. and B.G.; visualization, M.C. and B.G.; supervision, M.C. and B.G.; project administration, M.C. and B.G.; funding acquisition, M.C. and B.G. All authors have read and agreed to the published version of the manuscript.

Funding: This research received no external funding.

Data Availability Statement: The datasets generated during and/or analyzed during the current study are available from the corresponding author on reasonable request.

Conflicts of Interest: The authors declare no conflict of interest.

Abbreviations

The abbreviations in this paper are given below:

ε	Perturbation parameter
C	Generic positive constant
λ	Real parameter
h_i	Mesh step size
x_i	Mesh node point
ω_N	Non-uniform mesh
σ_1 and σ_2	Mesh transition points
e^N	Maximum error
p^N	Order of convergence
L	Differential operator
T	Volterra integral operator
S	Fredholm integral operator
u_i	Exact solution of the presented problem
y_i	Approximate solution of the difference problem
R_i	Remainder term
z_i	Error function

References

1. Amin, R.; Nazir, S.; Garcia-Magarino, I. A collocation method for numerical solution of nonlinear delay integro-differential equations for wireless sensor network and internet of things. *Sensors* **2020**, *20*, 1962. [CrossRef] [PubMed]
2. Dawood, L.A.; Hamoud, A.; Mohammed, N.M. Laplace discrete decomposition method for solving nonlinear Volterra-Fredholm integro-differential equations. *J. Math. Comput. Sci.* **2020**, *21*, 158–163. [CrossRef]
3. Kashkaria, B.S.H.; Syam, M.I. Evolutionary computational intelligence in solving a class of nonlinear Volterra-Fredholm integro-differential equations. *J. Comput. Applied Math.* **2017**, *311*, 314–323. [CrossRef]
4. Bellomo, N.; Firmani, B.; Guerri, L. Bifurcation analysis for a nonlinear system of integro-differential equations modelling tumor-immune cells competition. *Appl. Math. Lett.* **1999**, *12*, 39–44. [CrossRef]
5. Guan, L.; Prieur, C.; Zhang, L.; Prieur, C.; Georges, D.; Bellemain, P. Transport effect of Covid-19 pandemic in France. *Annu. Rev. Control* **2020**, *50*, 394–408. [CrossRef]
6. Köhler-Rieper, F.; Röhl, C.H.F.; De Michecli, E. A novel deterministic forecast model for the Covid-19 epidemic based on a single ordinary integro-differential equations. *Eur. Phys. J. Plus* **2020**, *135*, 599. [CrossRef]
7. Hamoud, A.A.; Bani Issa, M.; Ghadle, K.P. Existence and uniqueness results for nonlinear Volterra-Fredholm integro-differential equations. *Nonlinear Funct. Anal. Appl.* **2018**, *23*, 797–805.
8. Hamoud, A.; Mohammed, N.; Ghadle, K. Existence and uniqueness results for Volterra-Fredholm integro-differential equations. *Adv. Theory Nonlinear Anal. Appl.* **2020**, *4*, 361–372. [CrossRef]
9. Al-Ahmad, S.; Sulaiman, I.M.; Nawi, M.M.A.; Mamat, M.; Ahmad, M.Z. Analytical solution of systems of Volterra integro-differential equations using modified differential transform method. *J. Math. Comput. Sci.* **2022**, *26*, 1–9. [CrossRef]
10. Bani Issa, M.S.H.; Hamoud, A.A. Solving systems of Volterra integro-differential equations by using semi analytical techniques. *Technol. Rep. Kansai Univ.* **2020**, *62*, 685–690.
11. Tahernezad, T.; Jalilian, R. Exponential spline for the numerical solutions of linear Fredholm integro-differential equations. *Adv. Differ. Equations* **2020**, *141*, 1–15. [CrossRef]
12. Segni, S.; Ghiat, M.; Guebbai, H. New approximation method for Volterra nonlinear integro-differential equations. *Asian-Eur. J. Math.* **2019**, *12*, 1950016. [CrossRef]

13. Alvandi, A.; Paripour, M. The combined reproducing kernel method and Taylor series for handling nonlinear Volterra integro-differential equations with derivative type kernel. *Appl. Math. Comput.* **2019**, *355*, 151–160. [CrossRef]
14. Amin, R.; Maharq, I.; Shah, K.; Elsayed, F. Numerical solution of the second order linear and nonlinear integro-differential equations using Haar wavelet method. *Arab. J. Basic Appl. Sci.* **2021**, *28*, 1–19. [CrossRef]
15. Swaidan, W.; Ali, H.S. A computational method for nonlinear Fredholm integro-differential equations using Haar wavelet collocation points. *J. Physics Conf. Ser.* **2021**, *1*, 012032. [CrossRef]
16. Issa, K.; Salehi, F. Approximate solution of perturbed Volterra-Fredholm integro-differential equations by Chebyshev Galerkin method. *J. Math.* **2017**, *2017*, 8213932. [CrossRef]
17. Basirat, B.; Shahdadi, M.A. Numerical solution of nonlinear integro-differential equations with initial conditions by Bernstein Operational matrix of derivative. *Int. J. Mod. Nonlinear Theory Appl.* **2013**, *2*, 141–149. [CrossRef]
18. Cakir, M.; Gunes, B.; Duru, H. A novel computational method for solving nonlinear Volterra integro-differential equation. *Kuwait J. Sci.* **2021**, *48*, 31–40. [CrossRef]
19. Cimen, E.; Yatar, S. Numerical solution of Volterra integro-differential equtaion with delay. *J. Math. Comput. Sci.* **2020**, *20*, 255–263. [CrossRef]
20. Chen, J.; He, M.; Huang, Y. A fast multiscale Galerkin method for solving second order linear Fredholm integro-differential equation with Dirichlet boundary conditions. *J. Comput. Appl. Math.* **2020**, *364*, 112352. [CrossRef]
21. Hesameddini, E.; Riahi, M. Galerkin matrix method and its convergence analysis for solving system of Volterra-Fredholm integro-differential equations. *Iran. J. Sci. Technol. Sci.* **2019**, *43*, 1203–1214. [CrossRef]
22. Ghomanjani, F. Numerical solution for nonlinear Volterra integro-differential equations. *Palest. J. Math.* **2020**, *9*, 164–169.
23. Cao, Y.; Nikan, O.; Avazzadeh, Z. A localized meshless technique for solving 2D nonlinear integro-differential equation with multi-term kernels. *Appl. Numer. Math.* **2023**, *183*, 140–156. [CrossRef]
24. Jafarzadeh, Y.; Ezzati, R. A new method for the solution of Volterra-Fredholm integro-differential equations. *Tblisi Math. J.* **2019**, *12*, 59–66. [CrossRef]
25. Sharif, A.A.; Hamoud, A.A.; Ghadle, K.P. Solving nonlinear integro-differential equations by using numerical techniques. *Acta Univ. Apulensis* **2020**, *61*, 43–53.
26. Shoushan, A.F.; Al-Humedi, H.O. The numerical solutions of integro-differential equations by Euler polynomials with least-squares method. *Polarch J. Archaeol. Egypt/Egyptol.* **2021**, *18*, 1740–1753.
27. Iragi, B.C.; Munyakazi, J.B. New parameter-uniform discretizations of singularly perturbed Volterra integro-differential equations. *Appl. Math. Int. Sci.* **2018**, *12*, 517–529. [CrossRef]
28. Iragi, B.C.; Munyakazi, J.B. A uniformly convergent numerical method for a singularly perturbed Volterra integro-differential equation. *Int. J. Comput. Math.* **2020**, *97*, 759–771. [CrossRef]
29. Kudu, M.; Amirali, I.; Amiraliyev, G.M. A finite difference method for a singularly perturbed delay integro-differential equations. *J. Of Computational Appl. Math.* **2016**, *308*, 379–390. [CrossRef]
30. Yapman, Ö.; Amiraliyev, G.M.; Amirali, I. Convergence analysis of fitted numerical method for a singularly perturbed nonlinear Volterra integro-differential equation with delay. *J. Comput. And Applied Math.* **2019**, *355*, 301–309. [CrossRef]
31. Amiraliyev, G.M.; Yapman, Ö.; Kudu, M. A fitted approximate method for a Volterra delay-integro-differential equation with initial layer. *Hacet. J. Math. Stat.* **2019**, *48*, 1417–1429. [CrossRef]
32. Mbroh, N.A.; Noutchie, S.C.O.; Massoukou, R.Y.M. A second order finite difference scheme for singularly perturbed Volterra integro-differential equation. *Alex. Eng. J.* **2020**, *59*, 2441–2447. [CrossRef]
33. Yapman, Ö.; Amiraliyev, G.M. A novel second order fitted computational method for a singularly perturbed Volterra integro-differential equation. *Int. J. Comput. Math.* **2019**, *97*, 1293–1302. [CrossRef]
34. Tao, X.; Zhang, Y. The coupled method for singularly perturbed Volterra integro-differential equations. *Adv. Differ. Equations* **2019**, *217*, 2139. [CrossRef]
35. Panda, A.; Mohapatra, J.; Amirali, I. A second-order post-processing technique for singularly perturbed Volterra integro-differential equations. *Mediterr. J. Math.* **2021**, *18*, 1–25. [CrossRef]
36. Amiraliyev, G.M.; Durmaz, M.E.; Kudu, M. Uniform convergence results for singularly perturbed Fredholm integro-differential equation. *J. Of Mathematical Anal.* **2018**, *9*, 55–64.
37. Amiraliyev, G.M.; Durmaz, M.E.; Kudu, M. Fitted second order numerical method for a singularly perturbed Fredholm integro-differential equations. *Bull. Belg. Math. Soc. Simon Stevin* **2020**, *27*, 71–88. [CrossRef]
38. Cimen, E.; Cakir, M. A uniform numerical method for solving singularly perturbed Fredholm integro-differential problem. *Comput. Appl. Math.* **2021**, *40*, 1–14. [CrossRef]
39. Durmaz, M.E.; Amiraliyev, G.M. A robust numerical method for a singularly perturbed Fredholm integro-differential equation. *Mediterr. J. Math.* **2021**, *18*, 1–17. [CrossRef]
40. Cakir, M.; Gunes, B. Exponentially fitted difference scheme for singularly perturbed mixed integro-differential equations. *Georgian Math. J.* **2022**, *29*, 193–203. [CrossRef]
41. Cakir, M.; Gunes, B. A new difference method for the singularly perturbed Volterra-Fredholm integro-differential equations on a Shishkin mesh. *Hacet. J. Math. Stat.* **2022**, *51*, 787–799.
42. Amiraliyev, G.M.; Durmaz, M.E.; Kudu, M. A numerical method for a second order singularly perturbed Fredholm integro-differential equation. *Miskolc Math. Notes* **2021**, *22*, 37–48.

43. Boglaev, I.P. Approximate solution of a nonlinear boundary value problem with a small parameter for the highest-order differential. *USSR Comput. Math. Math. Phys.* **1984**, *24*, 30–35. [CrossRef]
44. Amiraliyev, G.M.; Mamedov, Y.D. Difference schemes on the uniform mesh for singularly perturbed pseudo-parabolic equations. *Tr. J. Math.* **1995**, *19*, 207–222.
45. Samarski, A.A. *The Theory of Difference Schemes*; M.V. Lomonosov State University: Moscow, Russia, 2021.